

Analytical Methods

Accepted Manuscript



This is an *Accepted Manuscript*, which has been through the Royal Society of Chemistry peer review process and has been accepted for publication.

Accepted Manuscripts are published online shortly after acceptance, before technical editing, formatting and proof reading. Using this free service, authors can make their results available to the community, in citable form, before we publish the edited article. We will replace this *Accepted Manuscript* with the edited and formatted *Advance Article* as soon as it is available.

You can find more information about *Accepted Manuscripts* in the [Information for Authors](#).

Please note that technical editing may introduce minor changes to the text and/or graphics, which may alter content. The journal's standard [Terms & Conditions](#) and the [Ethical guidelines](#) still apply. In no event shall the Royal Society of Chemistry be held responsible for any errors or omissions in this *Accepted Manuscript* or any consequences arising from the use of any information it contains.

ARTICLE

Highly sensitive electrochemical sensor for dopamine with a double-stranded deoxyribonucleic acid/gold nanoparticle/graphene modified electrode

Cite this: DOI: Wencheng Wang^a, Yong Cheng^b, Lijun Yan^a, Huanhuan Zhu^b, Guangjiu Li^{b*}, Jing Li^a, Wei Sun^{a*}

^aCollege of Chemistry and Chemical Engineering, Hainan Normal University, Haikou 571158, China;
^bCollege of Chemistry and Molecular Engineering, Qingdao University of Science and Technology, Qingdao 266042, China

Received
Accepted

DOI:

www.rsc.org/

In this paper a novel electrochemical sensor was fabricated for the sensitive detection of dopamine (DA). By using a carbon ionic liquid electrode (CILE) as substrate electrode, graphene (GR), gold nanoparticle (AuNP) and double-stranded deoxyribonucleic acid (dsDNA) were electrodeposited on the surface of CILE step-by-step to get the modified electrode (dsDNA/Au/GR/CILE). Due to the presence of various modifiers on the electrode surface, the modified electrode exhibited specific synergistic effects, such as high conductivity and large surface of GR, good conductivity and biocompatibility of AuNP, and the specific binding effect of dsDNA with target analyte DA. Cyclic voltammetric studies indicated that a pair of well-define redox peaks of DA appeared on dsDNA/Au/GR/CILE in pH 6.0 phosphate buffer solution and electrochemical behaviors of DA were carefully investigated. Under the optimal conditions the oxidation peak current of DA was linearly related to DA concentration in the range from 0.04 $\mu\text{mol L}^{-1}$ to 0.6 mmol L^{-1} with a detection limit of 19.0 nmol L^{-1} (3σ). The modified electrode displayed excellent selectivity and repeatability, which was further used to detect DA content in the drug samples with satisfactory results.

Introduction

As a two-dimensional layered nanosheet, graphene (GR) has attracted extensive scientific interests due to its unique electrical, optical and mechanical properties, as well as its potential applications in various fields such as electronics, supercapacitors, sensors and composite materials.¹ Different kinds of methods have been proposed for the synthesis of GR, among them the chemical reduction of graphene oxide (GO) obtained from ultrasonic exfoliation of oxidized graphite is the most convenient procedure to prepare large quantities of GR nanosheets.² Due to its specific electrochemical properties, GR has been used for the electrode modification and electrochemical sensing. However, due to the partly aggregation of GR nanosheets on the electrode surface, drop-casting method for the electrode modification, which is commonly used for the preparation of GR modified electrode, exhibits poor reproducibility. Recently direct electrodeposition of GO from the solution to the electrode surface has been used for the preparation of GR-based electrode, which exhibits the advantages

including green nature, controllable process without the usage of toxic reagents. By using different electrochemical techniques such as voltammetry or potentiostatic method, GO can be electrochemically reduced with a layer of GR formed on the electrode surface.³ Furthermore, other kinds of metal nanoparticles can be further deposited on the GR surface to get the composite with multi-functions.⁴ Among them gold nanoparticle (AuNP) is one of the most studied nanomaterials due to its remarkable properties. Pingarron et al. reviewed the applications of AuNP based electrochemical biosensors.⁵ The presence of AuNP on the electrode surface can provide a suitable microenvironment for biomolecules and facilitate the electron transfer rate, which are suitable for the fabrication of different kinds of electrochemical biosensors. Hu et al. applied AuNP decorated GR sheets for the label-free electrochemical impedance DNA hybridization biosensing.⁶ A dendritic gold and electrochemically reduced GR modified electrode was also fabricated as the DNA sensor for the electrochemical detection of *Listeria monocytogenes*.⁷ AuNP and

GR nanocomposite had also been fabricated by different methods,⁸ which could be applied to the electrochemical detection of electroactive compounds.⁹

Deoxyribonucleic acid (DNA) is one of the most important biomacromolecule that can be used in different fields of electrochemical sensors. By selecting specific ssDNA sequence as the recognition element, ssDNA modified electrodes have been widely used as the electrochemical DNA biosensor for gene detection over the last decade,^{10,11} which exhibit the practical applications in both molecular biology and modern biomedical engineering. Also DNA recognition layers on the electrode surface can be applied to the research fields such as DNA damage, genetic diseases, drug monitoring and environmental research.^{12,13} Due to the high charge density of the DNA helix and the binding ability to various molecules, DNA can also be served as modifier on the electrode with good selectivity and sensitivity. Electrochemical sensors based on DNA recognition had been reported for the detection of dopamine (DA), norepinephrine and uric acid in the presence of ascorbic acid (AA).^{14,15}

In recent year a new carbon composite electrode, which is prepared by using ionic liquid (IL) as an efficient binder in place of nonconductive organic binders in carbon paste electrode (CPE), has been devised and commonly named as carbon ionic liquid electrode (CILE).¹⁶ As a new type of working electrode with the advantages such as easy preparation, good reversibility, high sensitivity and the ability to lower the overpotential of electroactive compounds, CILE has aroused great interests in the field of electroanalysis.¹⁷ The presence of IL on the surface of carbon powder can provide a specific interface for the electrochemical reaction with fast electron transfer rate and accumulation affects. Recently, chemically modified CILE has also been reported and used for the electrochemical sensors, which combine the native properties of the modifiers and CILE simultaneously. Our group applied different kinds of nanomaterials modified CILE for the realization of protein electrochemistry.^{18,19} The co-contributions of CILE and modifiers on the electrode surface can enhance the electrochemical responses of the analyte with improved sensitivity.

In this paper a CILE was fabricated with N-hexylpyridinium hexafluorophosphate (HPPF₆) as the modifier, which was further modified by GR, AuNP and dsDNA step-by-step to get a new multilayer modified electrode (dsDNA/Au/GR/CILE). Due to the synergistic effects of the materials used, such as the excellent conductivity of AuNP and GR, and the recognition effect of dsDNA, the modified electrode exhibited excellent electrochemical performances. Electrochemical responses of DA were greatly enhanced on dsDNA/Au/GR/CILE and electrochemical behaviors of DA were carefully investigated. Based on the oxidation peak of DA on the modified electrode a sensitive differential pulse voltammetric method for DA determination was further developed and applied to the real drug samples detection with satisfactory results.

Experimental

Apparatus and chemicals

This journal is © The Royal Society of Chemistry 2014

All the electrochemical experiments were carried out on a CHI 750B electrochemical workstation (Shanghai CH Instrument, China). A conventional three-electrode system was used with a dsDNA/Au/GR/CILE as working electrode, a platinum wire as auxiliary electrode and a saturated calomel electrode (SCE) as reference electrode. Scanning electron microscopy (SEM) was obtained by a JSM-7500F scanning electron microscope (Japan Electron Company, Japan).

HPPF₆ (>99%, Lanzhou Greenchem. ILS. LICP. CAS., China), DA (Aladdin Reagent Ltd. Co., China), graphite powder (average particle size 30 μm, Shanghai Colloid Chemical Ltd. Co., China), chloroauric acid (HAuCl₄, Shanghai Chemical Plant, China), GO (Taiyuan Tanmei Ltd. Co., China) and herring sperm double-stranded deoxyribonucleic acid (dsDNA, Shanghai Kayon Biochem. Ltd. Co., China) were used as received. 0.1 mol L⁻¹ phosphate buffer solutions (PBS) with various pH values were used as the supporting electrolyte. All the other chemicals used were of analytical reagent grade and doubly distilled water was used in the experiments.

Preparation of the modified electrode

HPPF₆ based CILE was fabricated according to the reported procedure.²⁰ Prior to use a mirror-like surface was obtained by polishing the electrode on a weighing paper. GR modified CILE was fabricated by placing newly prepared CILE in a 1.0 mg mL⁻¹ GO dispersion solution with magnetic stirring and N₂ bubbling. After electrodeposition at -1.3 V for 300 s, a stable electrochemical reduced GR film was formed on the CILE surface. The resulted GR/CILE was rinsed with doubly distilled water and dried in nitrogen atmosphere. Then AuNP was further electrodeposited on the surface of GR/CILE by applying the potential of -0.4 V for 300 s in a 5.0 mmol L⁻¹ HAuCl₄ solution. The resulted Au/GR/CILE was rinsed with doubly distilled water and dried in air for further modification. Lastly dsDNA was electrodeposited on the surface of Au/GR/CILE through a 0.1 mg L⁻¹ dsDNA solution (in pH 7.0 PBS) at a constant potential of +0.5 V for 1200 s. The modified electrode was denoted as dsDNA/Au/GR/CILE and stored at 4 °C refrigerator when not in use.

Results and discussion

Characteristics of the modified electrodes

The characteristics of the modified electrodes were investigated to show the interfacial information. Firstly, SEM is used to show the top views of different modified electrodes with the results shown in Fig. 1. On the CILE surface the irregularly micrometer-sized graphite powder was connected by high viscosity IL with a continuous interface appeared (Fig. 1A). After the first electrodeposition step the typical lamellar structure of GR nanosheets could be observed (Fig. 1B). Electrochemical reduction is a convenient method to get the GR film directly on the electrode and the formed GR layers are beneficial in maintaining a larger surface area,²¹ which can provide more sites for the further electrodeposition of AuNP. The morphology of Au/GR/CILE (Fig.

1C) clearly indicated that nanosized gold could be easily observed on the lamellar structure of GR. The presence of GR sheets could absorb more cationic gold ions before electrochemical reduction and a homogeneous nanocomposite could be formed on the interface with a further increase of surface area. After the electroadsorption of dsDNA the interface changed greatly, indicating the successful immobilization of dsDNA on the electrode. DNA is negatively charged due to its phosphate structure, which can be adsorbed on the electrode surface at the positive potential with a layer of dsDNA formed on the electrode.¹³

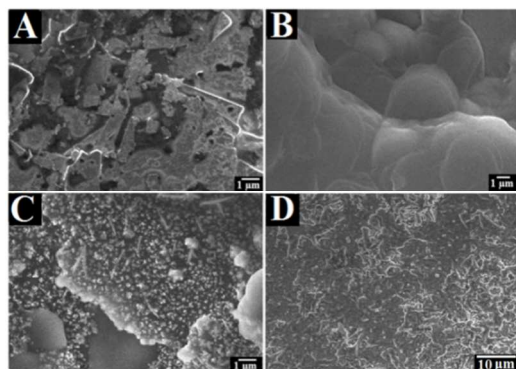


Fig. 1 SEM images of (A) CILE, (B) GR/CILE, (C) Au/GR/CILE and (D) dsDNA/Au/GR/CILE.

Electrochemical performances of different modified electrodes were further evaluated. Cyclic voltammograms were recorded in a $1.0 \text{ mmol L}^{-1} [\text{Fe}(\text{CN})_6]^{3-}$ solution with a pair of well-defined redox peaks appeared on all the electrodes (shown in Fig.2A), indicating the modified electrodes exhibited good performances. It can be seen that the redox peak currents increased gradually with the gradually modification by different modifiers on the electrode surface. On CILE the smallest redox peak currents appeared (curve a) and that of GR/CILE increased (curve b), which was attributed to the presence of high conductive GR on CILE with increased surface area. On Au/GR/CILE the biggest redox peak currents appeared with the smallest peak-to-peak separation (ΔE_p) value of 0.066 V (curve d), which suggested that the presence of GR-Au composite on the electrode surface could further accelerate the electron transfer due to the high conductivity. Compared with that of Au/GR/CILE, the redox peak currents on dsDNA/Au/GR/CILE decreased (curve c), demonstrating that dsDNA had been successfully immobilized on the electrode surface. The negatively charged phosphate skeletons of dsDNA on Au/GR/CILE had a repulsive force to $[\text{Fe}(\text{CN})_6]^{3-}$ in the solution, so the current response of $[\text{Fe}(\text{CN})_6]^{3-/4-}$ on dsDNA/Au/GR/CILE was decreased. Electrochemical impedance spectrum (EIS) can also provide interfacial information during the modification process. By using a $10.0 \text{ mmol L}^{-1} [\text{Fe}(\text{CN})_6]^{3-/4-}$ solution as the electrochemical probe, the Nyquist plots of different modified electrodes were recorded with the results shown in Fig. 2B. The electron transfer resistance (R_{et}) of CILE (curve a), GR/CILE (curve b) and Au/GR/CILE (curve d) were got as 151.2Ω , 66.78Ω and 21.36Ω , respectively. The gradually decrease of R_{et} value proved that the presence of high conductive GR and AuNP on the electrode surface could

greatly decrease the interfacial resistance. While on dsDNA/Au/GR/CILE the R_{et} value was increased to 51.21Ω (curve c), which was bigger than that of Au/GR/CILE. The result may be due to the presence of negatively charged dsDNA on the electrode surface hindered the electron transfer of $[\text{Fe}(\text{CN})_6]^{3-/4-}$. All the results were in good agreement with that of cyclic voltammetric data, which indicated that the modified electrodes were successfully fabricated.

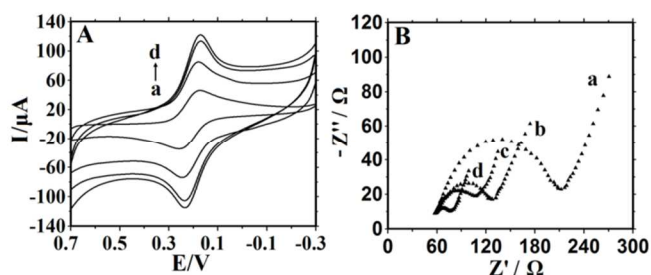


Fig. 2 (A) Cyclic voltammograms of different modified electrodes in a $1.0 \text{ mmol L}^{-1} \text{K}_3[\text{Fe}(\text{CN})_6]$ and $0.5 \text{ mol L}^{-1} \text{KCl}$ solution with scan rate as 100 mV s^{-1} ; (B) Electrochemical impedance spectra of different modified electrodes in $10.0 \text{ mmol L}^{-1} [\text{Fe}(\text{CN})_6]^{3-/4-}$ and $0.1 \text{ mol L}^{-1} \text{KCl}$ solution with the frequently swept from 10^5 to 0.1 Hz . From a to d were CILE, GR/CILE, dsDNA/Au/GR/CILE and Au/GR/CILE, respectively.

Electrochemical behaviors of DA on the modified electrodes

Cyclic voltammograms of DA at different modified electrodes were recorded and shown in Fig. 3. Due to the electroactivity of DA a pair of redox peak appeared on all the electrodes, which was in accordance with the reported electrochemical behavior of DA.²² On bare CILE (curve a) DA exhibited a pair of draw-out cyclic voltammetric peaks. The oxidation peak (E_{pa}) appeared at 0.35 V and the reduction peak (E_{pc}) at 0.078 V with the ΔE_p as 0.272 V . While on GR/CILE (curve b) a couple of redox peaks appeared at 0.26 V (E_{pa}) and 0.15 V (E_{pc}) with the ΔE_p as 0.11 V . The redox peak currents increased for 2.6 fold, which could be attributed to the presence of GR with high conductivity and certain electrocatalytic activity. The redox peak currents were further increased on Au/GR/CILE with the ΔE_p value decreased to 0.071 V (curve c), indicating the synergistic effects of GR and Au NP. The presence of Au-GR nanocomposite exhibits the properties including the large surface area of GR, the good conductivity of Au and GR, and their co-contribution. While on dsDNA/Au/GR/CILE a couple of well-defined and sharp cyclic voltammetric peaks appeared at 0.24 V (E_{pa}) and 0.17 V (E_{pc}). The biggest redox peak currents and the smallest ΔE_p value of 0.070 V indicated that the presence of dsDNA further increased the electrochemical responses of DA. Due to the electrostatic interactions between the positively charged DA and the negatively charged phosphate backbone of dsDNA, as well as the excellent conductivity of Au/GR/CILE, more DA could be accumulated on the electrode surface with the increase of DA concentration, and then the electrochemical responses were enhanced greatly. Therefore by using dsDNA/Au/GR/CILE as the working electrode, a sensitive

electrochemical method for the DA detection was further established.

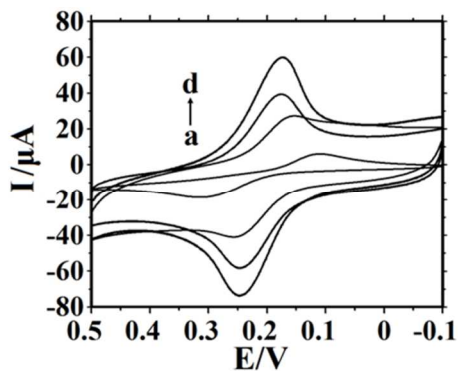


Fig. 3 Cyclic voltammograms of 1.0×10^{-4} mol L^{-1} DA on (a) CILE, (b) GR/CILE, (c) Au/GR/CILE and (d) dsDNA/Au/GR/CILE in pH 6.0 PBS. Scan rate: 100 mV s^{-1} .

Effect of buffer pH

The effect of buffer pH on the electrochemical reaction of DA was investigated with the typical voltammograms shown in Fig. 4A. It can be seen that the electrochemical responses of DA on dsDNA/Au/GR/CILE showed a strong dependence with the buffer pH. The relationships of the formal peak potential (E^0) and the oxidation peak current with pH were further constructed with the results shown in Fig. 4B and 4C. The linear relationship between E^0 and pH was plotted with the linear regression equation as $E^0(\text{V}) = -0.0568 \text{ pH} + 0.554$ ($\gamma=0.997$). The slope value of $-0.0568 \text{ V pH}^{-1}$ was close to the theoretical value of -0.059 V pH^{-1} , indicated that the same amounts of electrons and protons took part in the electrode reaction. The oxidation peak current increased gradually with the increase of pH from 4.5 to 6.0, reached a maximum value at the pH value of 6.0 and then decreased with the further increase of buffer pH. So pH 6.0 was selected for further investigation.

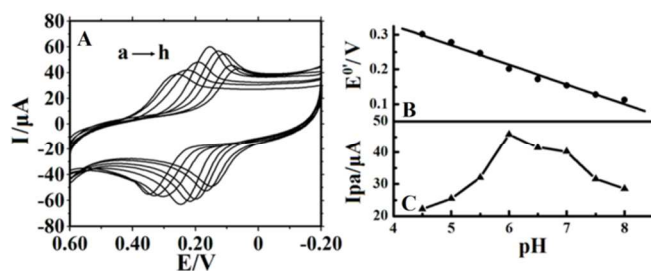


Fig. 4 (A) Cyclic voltammograms of 1.0×10^{-4} mol L^{-1} DA on dsDNA/Au/GR/CILE with different pH PBS (from a to h are 4.5, 5.0, 5.5, 6.0, 6.5, 7.0, 7.5, 8.0), at scan rate of 100 mV s^{-1} ; (B) The relationship between the formal peak potential (E^0) and pH; (C) The relationship between the oxidation peak current (I_{pa}) and pH.

Influence of scan rate

The influence of scan rate on the electrochemical responses of DA was further investigated by cyclic voltammetry with the results shown in Fig. S1A. With the increase of scan rate the redox peak

currents increased gradually in the range from 0.01 to 0.5 V s^{-1} . Also the oxidation peak potential shifted to the positive direction and the reduction peak potential to the negative direction with the increase of the ΔE_p value, indicating a quasi-reversible electrochemical process. A good linear relationship between the redox peak current (I_p) and the square root of scan rate ($v^{1/2}$) were plotted (as shown in Fig. S1B) with the linear regression equations as $I_{pa}(\mu\text{A}) = -93.68 v^{1/2} (\text{V s}^{-1}) - 0.829$ ($\gamma=0.999$) and $I_{pc}(\mu\text{A}) = 133.46 v^{1/2} (\text{V s}^{-1}) - 9.214$ ($\gamma=0.999$), which indicated a diffusional-controlled process. The electron transfer kinetics of DA on dsDNA/Au/GR/CILE can be investigated by the following equations,²³

$$E_{pa} = E^0 + m[0.78 + \ln(D^{1/2}k_s^{-1}) - 0.5 \ln m] + \frac{m}{2} \ln v, m = \frac{RT}{(1-\alpha)nF} \quad (1)$$

$$E_{pc} = E^0 - m'[0.78 + \ln(D^{1/2}k_s^{-1}) - 0.5 \ln m'] - \frac{m'}{2} \ln v, m' = \frac{RT}{\alpha nF} \quad (2)$$

$$\log k_s = \alpha \log(1-\alpha) + (1-\alpha) \log \alpha - \log \frac{RT}{nFv} - \frac{(1-\alpha)\alpha F \Delta E_p}{2.3RT} \quad (3)$$

Where α is the charge transfer coefficient, n is the number of electrons transferred, k_s is the electron transfer rate constant, v is the scan rate, E^0 is the formal peak potential and F is the Faraday constant. The redox peak potential and $\ln v$ exhibited a good linear relationship (as shown in Fig. S1C) with the regression equations as $E_{pa}(\text{V}) = 0.0151 \ln v (\text{V s}^{-1}) + 0.0288$ ($\gamma=0.997$) and $E_{pc}(\text{V}) = -0.0128 \ln v (\text{V s}^{-1}) + 0.126$ ($\gamma=0.997$). According to the above equations, the electrochemical parameters were further calculated with the values of α , n and k_s as 0.541, 1.85, and 1.63 s^{-1} , respectively. The value of k_s was close to the reported value of 1.66 s^{-1} on layered double hydroxide (LDH) modified CILE²² and is bigger than some reported values,²⁴⁻²⁶ indicating a relative faster electron transfer process on dsDNA/Au/GR/CILE.

Interference

The influences of some coexisting substances such as inorganic ions and organic compounds that commonly existed in biological sample on the determination of 1.0×10^{-4} mol L^{-1} DA were investigated by cyclic voltammetry with the results listed in Table S1. It can be seen that most of them did not interfere with the determination, indicating the good selectivity of the modified electrode.

Electrochemical responses of DA in the presence of high concentrations AA on dsDNA/Au/GR/CILE were also studied by differential pulse voltammetry (DPV) with the voltammograms shown in Fig. 5. On dsDNA/Au/GR/CILE the oxidation peak of AA appeared at 0.034 V (curve a), and the mixture of AA and DA gave two oxidation peaks at the potentials of 0.034 and 0.199 V (curve b), respectively, which were attributed to the electrooxidation of AA and DA, respectively. The separation of the oxidation peak potential was calculated as 0.165 V, which was large enough for simultaneously determinations of DA and AA in the mixture solution.

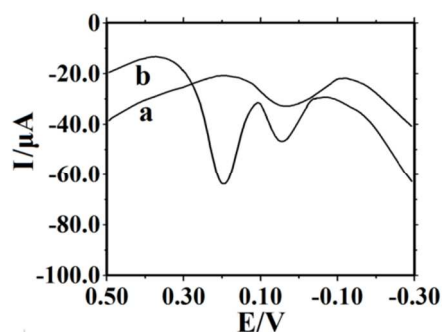


Fig. 5 Differential pulse voltammograms of 1.0×10^{-3} mol L^{-1} AA (a); the mixed solution of 1.0×10^{-3} mol L^{-1} AA and 1.0×10^{-4} mol L^{-1} DA (b) on dsDNA/Au/GR/CILE in pH 6.0 PBS.

Calibration curve

Due to the high sensitivity and good peak-shape curve, DPV was adopted for the quantitative determination of DA and the typical voltammograms were shown in Fig. 6A. Under the optimal conditions the oxidation peak currents increased linearly with DA concentrations in the range from 0.070 to 80.0 $\mu\text{mol L}^{-1}$ and 80.0 to 600.0 $\mu\text{mol L}^{-1}$ (Fig. 6B) with the linear regression equations as $I_{pa}(\mu\text{A}) = 2.667 + 0.695 C (\mu\text{mol L}^{-1})$ ($\gamma = 0.996$) and $I_{pa}(\mu\text{A}) = 47.0 + 0.101 C (\mu\text{mol L}^{-1})$ ($\gamma = 0.997$), respectively. The detection limit was calculated as 19.0 nmol L^{-1} (3σ). The comparisons of the analytical parameters for DA detection by different modified electrodes were summarized in Table 1. It can be seen that the proposed method gave a higher sensitivity with broader linear range for DA detection, which could be attributed to the synergistic effects of dsDNA, AuNP and GR on the electrode surface. The modified electrode exhibited good reproducibility and the relative standard deviation (RSD) of 11 successive detections for 1.0×10^{-4} mol L^{-1} DA was 2.6%. Five modified electrodes were fabricated independently for the detection of 1.0×10^{-4} mol L^{-1} DA, which gave a satisfactory RSD value of 1.9%, indicating the good repeatability.

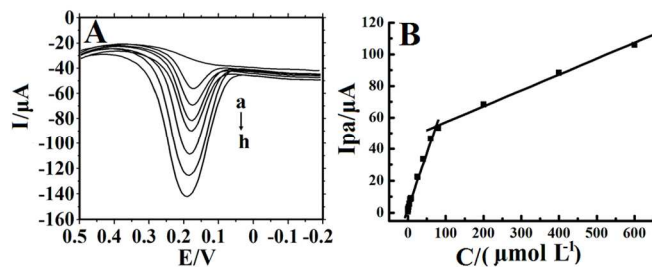


Fig. 6 (A) Differential pulse voltammograms of various concentrations DA on dsDNA/Au/GR/CILE in pH 6.0 PBS (from a to h 0.0, 20.0, 40.0, 60.0, 80.0, 200.0, 400.0, 600.0 $\mu\text{mol L}^{-1}$); (B) The relationship of the oxidation peak current with the DA concentration.

Table 1 Comparison of the analytical performances for DA detection on different modified electrodes

Electrodes	Linear range ($\mu\text{mol L}^{-1}$)	LOD ($\mu\text{mol L}^{-1}$)	Refs
LDH/CILE	10.0-1100.0	5.0	[22]
SWCNT/GCE	0.01-0.2	0.015	[27]
PtAu/GCE	24.0-384.0	5.0	[28]
DNA/Pp-ABSA/GCE	0.19-13.0	0.088	[29]
Graphene/GCE	4.0-100.0	2.64	[30]
Nafion/clay/GCE	0-6.0	0.027	[31]
CNT-TNCPE	0.1-80.0	0.08	[32]
CNT-GCE	0.016-60.0	0.008	[33]
TCPP/CCG/GCE	0.1-1.0	0.022	[34]
DNA/PPyox/CFE	0.3-10.0	0.08	[35]
ITO electrode	/	0.001	[36]
GCE	4.5-400.0	2.3	[37]
Qu/GH/GCE	/	0.01	[38]
RGO-Pd-NPs/GCE	1-150.0	0.233	[39]
{AuNPs/RGO} ₂₀ /GCE	1-60	0.02	[40]
DNA/Au/GR/CILE	0.08-600	0.019	This paper

Sample determination

The proposed method was further applied to the determination of the content of DA in injection sample, which was purchased from Jiangsu Yabang Pharmacy Limited Company (100423) with the specified amount as 10.0 mg mL^{-1} . The samples were diluted to 10.0 mL by water and 60.0 μL of the diluted sample was detected by the experimental procedure with the standard addition method. The analytical results were listed in Table S2, which indicated that the determination was satisfactory with the recovery in the range of 97.4 % to 102.2 %. So the proposed electrode could be efficiently used for the determination of DA in the injection samples.

Conclusion

A new kind of chemically modified electrode was prepared by using electrodeposited GR, AuNP and dsDNA modified CILE, which exhibited the synergistic effects of the modifiers used. GR nanosheets have large surface area with high conductivity, which can be used for the further decoration of nanoparticles. AuNP exhibits excellent conductivity and good biocompatibility, which is suitable for the further immobilization of biomolecules with bioactivity retained. As a molecular transducer with double stranded structure, dsDNA can interact with DA and accumulate more DA on the electrode surface. Based on the co-contributions of the modifiers on the electrode, DA can be accumulated and take place faster electron transfer reaction with a pair of well-defined redox peaks appeared. Under the selected conditions, the oxidation peak current was proportional to the DA concentration in the range from 0.07 $\mu\text{mol L}^{-1}$ to 600.0 $\mu\text{mol L}^{-1}$ with the detection limit as

19.0 nmol L⁻¹ (3σ). The proposed method was further applied to DA injection samples detection with good recovery, indicating that the potential applications of the modified electrode.

Acknowledgements

We acknowledge the financial support of the National Natural Science Foundation of China (No. 21365010, 51365008), the Natural Science Foundation of Shandong Province (ZR2013BM014) and the Nature Science Foundation of Hainan Province (213015, 214022).

References

- 1 K. S. Novoselov, D. Jiang, F. Schedin, T. J. Booth, V. V. Khotkevich, S. V. Morozov, A. K. Geim, *PANS*, 2005, **102**, 10451.
- 2 M. Pumera, *Chem. Soc. Rev.*, 2010, **39**, 4146.
- 3 M. Zhou, Y. L. Wang, Y. M. Zhai, J. F. Zhai, W. Ren, F. Wang, S. J. Dong, *Chem. Eur. J.*, 2009, **15**, 6116.
- 4 C. B. Liu, K. Wang, S. L. Luo, Y. H. Tang, L. Y. Chen, *Small*, 2011, **7**, 1203.
- 5 J. M. Pingarron, P. Yanez-Sedeno, A. Gonzalez-Cortes, *Electrochim. Acta*, 2008, **53**, 5848.
- 6 Y. W. Hu, S. C. Hua, F. H. Li, Y. Y. Jiang, X. X. Bai, D. Li, L. Niu, *Biosens. Bioelectron.*, 2011, **26**, 4355.
- 7 W. Sun, X. W. Qi, Y. Y. Zhang, H. R. Yang, H. W. Gao, Y. Chen, Z. F. Sun, *Electrochim. Acta*, 2012, **85**, 145.
- 8 G. Goncalves, P. A. A. P. Marques, C. M. Granadeiro, H. I. S. Nogueira, M. K. Singh, J. Gracio, *Chem. Mater.*, 2009, **21**, 4796.
- 9 S. Hu, Y. H. Wang, X. Z. Wang, L. Xu, J. Xiang, W. Sun, *Sens. Actuators B*, 2012, **168**, 27.
- 10 M. I. Pividori, A. Merkoç, S. Alegret, *Biosens. Bioelectron.*, 2000, **15**, 291.
- 11 A. Liu, K. Wang, S. Weng, Y. Lei, L. Lin, W. Chen, X. Lin, Y. Chen, *Trends Anal. Chem.*, 2012, **37**, 101.
- 12 J. Wang, M. Chicharro, G. Rivas, X. H. Cai, N. Dontha, P. A. M. Farias, H. Shiraishi, *Anal. Chem.*, 1996, **68**, 2251.
- 13 X. Q. Lin, X. H. Jiang, L. P. Lu, *Biosens. Bioelectron.*, 2005, **20**, 1709.
- 14 X. Q. Lin, L. P. Lu, X. H. Jiang, *Microchim. Acta*, 2003, **143**, 229.
- 15 L. P. Lu, X. Q. Lin, *Anal. Sci.* 2004, **20**, 527.
- 16 M. Opallo, A. Lesniewski, *J. Electroanal. Chem.*, 2011, **656**, 2.
- 17 M. J. A. Shiddiky, A. A. J. Torriero, *Biosens. Bioelectron.*, 2011, **26**, 1775.
- 18 W. Sun, X. Q. Li, P. Qin, K. Jiao, *J. Phys. Chem. C*, 2009, **113**, 11294.
- 19 W. Sun, P. Qin, R. J. Zhao, K. Jiao, *Talanta*, 2010, **80**, 2177.
- 20 W. Sun, Y. Y. Duan, Y. Z. Li, T. R. Zhan, K. Jiao, *Electroanalysis*, 2009, **21**, 2667.
- 21 H. L. Guo, X. F. Wang, Q. Y. Qian, F. B. Wang, X. H. Xia, *ACS Nano*, 2009, **3**, 2653.
- 22 Z. H. Zhu, L. N. Qu, Y. Q. Guo, Y. Zeng, W. Sun, *Sens. Actuators B*, 2010, **151**, 146.
- 23 R. S. Nicholson, I. Shain, *Anal. Chem.*, 1964, **36**, 706.
- 24 J. M. Zen, A. S. Kumar, H. P. Chen, *Electroanalysis*, 2003, **15**, 1584.
- 25 C. Y. Hsu, V. S. Vasantha, P. Y. Chen, K. C. Ho, *Sens. Actuators B*, 2009, **137**, 313.
- 26 X. Zhou, N. Zheng, S. R. Hou, X. J. Li, Z. B. Yuan, *J. Electroanal. Chem.*, 2010, **642**, 30.
- 27 S. Alwarappan, G. D. Liu, C. Z. Li, *Nanomedicine: NBM*, 2010, **6**, 52.
- 28 S. Thiagarajan, S. M. Chen, *Talanta*, 2007, **74**, 212.
- 29 X. Q. Lin, G. F. Kang, L. P. Lu, *Bioelectrochemistry*, 2007, **70**, 235.
- 30 Y. R. Kim, S. Bong, Y. J. Kang, Y. Yang, R. K. Mahajan, J. S. Kim, H. Kim, *Biosens. Bioelectron.*, 2010, **25**, 2366.
- 31 J. M. Zen, P. J. Chen, *Anal. Chem.*, 1997, **69**, 5087.
- 32 S. Shahrokhian, H. R. Zare-Mehrjardi, *Electrochim. Acta*, 2007, **52**, 6310.
- 33 Y. Zhang, Y. Cai, S. Su, *Anal. Biochem.*, 2006, **350**, 285.
- 34 L. Wu, L. Y. Feng, J. S. Ren, X. G. Qu, *Biosens. Bioelectron.*, 2012, **34**, 57.
- 35 X. H. Jiang, X. Q. Lin, *Analyst*, 2005, **130**, 391.
- 36 B. Kim, S. Son, K. Lee, H. Yang, J. Kwak, *Electroanalysis*, 2012, **24**, 993.
- 37 M. Sabino, M. Begoña, J. Francisco, L. Beatriz, *Sensor Lett.*, 2011, **9**, 1670.
- 38 Z. H. Wang, J. F. Xia, L. Y. Zhu, X. Y. Chen, F. F. Zhang, S. Y. Yao, Y. Z. Xia, *Electroanalysis*, 2011, **23**, 2463.
- 39 S. Palanisamy, S. H. Ku, S. M. Chen, *Microchim. Acta*, 2013, **180**, 1037.
- 40 S. Liu, J. Yan, G. W. He, D. D. Zhong, J. X. Chen, L. Y. Shi, X. M. Zhou, H. J. Jiang, *J. Electroanal. Chem.*, 2012, **672**, 40.